Available online at www.eccomasproceedia.org
Eccomas Proceedia SMART (2023) 1732-1742

ECCOMAS
Proceedia

X ECCOMAS Thematic Conference on Smart Structures and Materials
SMART 2023
D.A. Saravanos, A. Benjeddou, N. Chrysochoidis and T. Theodosiou (Eds)

SHIFTING CORRECTION OF INTEGRATED DIC METHOD FOR MEASUREMENT OF RESIDUAL STRESS

MING-HSIANG SHIH*, WEN-PEI SUNG† AND SHIH-HENG TUNG#

* Department of Civil Engineering, National Chi Nan University
No.1, University Road, Puli, Nantou 545, Taiwan
e-mail: iloveaachen@gmail.com

† Department of Landscape Architecture, National Chin-Yi University of Technology
No.57, Sec. 2, Zhongshan Rd., Taiping Dist., Taichung 411030, Taiwan
email: drwpsung@gmail.com

Department of Civil and Environment Engineering, National University of Kaohsiung
700, Kaohsiung University Rd., Nanzih District, Kaohsiung 811, Taiwan
email: shtung@nuk.edu.tw

Abstract. This paper discusses current stress measurement techniques, specifically the hole-drilling method and blind hole-drilling method, which involve drilling a small hole to induce stress relaxation and measuring the deformation before and after drilling to infer the stress tensor. Relaxation strain measurement techniques, including strain gauge, interferometry, and image measurement methods, are necessary for successful application of these techniques. The aim of this study is to improve the accuracy of the image measurement method, making it a low-cost, high-precision, and highly mobile current stress measurement technique. Two strategies are proposed for this purpose. Firstly, the near-field image measurement accuracy is improved by addressing the distance variation between the camera and specimen caused by the drilling process. A camera translation method is proposed to eliminate this measurement error. Secondly, the identification theory for image recognition of current stress accuracy is improved. The accuracy of identifying the current stress is crucial for the accuracy of the measurement results. The Nelson strain field integrated digital image correlation method is applied to improve the accuracy of image recognition of current stress. The experimental results prove that the shifting correction method proposed in this paper can greatly eliminate the measurement error, reducing the measurement error of the residual stress from 4.5% to 1.57%. In terms of the sensitivity of the analysis parameter settings to measurement errors, the aperture is the most sensitive parameter and must be set very carefully. As for the location of the center of the hole and the range of the analysis integration, as long as they are properly coordinated, there is a large room for error tolerance. Through these strategies, this study aims to make the image measurement method a more effective, high-precision, and low-cost current stress measurement technique, which is expected to be more widely used in the future.

Key words: Residual Stress, Integrated Digital Image Correlation, Shifting Correction.

Peer-review under responsibility of the organizing committee of SMART 2023.
doi: 10.7712/150123.9944.444203

1 INTRODUCTION

The hole-drilling method is currently the most widely used residual stress measurement technique, owing to its high accuracy, low cost, and semi-destructive nature. By drilling a small hole on the plane of a workpiece with residual stress, stress is released and redistributed in the vicinity of the hole. Subsequently, three or more sets of strain gauges placed on the same circumference can be used to measure the corresponding radial strain data, enabling the estimation of the original stress state at the location of the hole.

The residual stress can be expressed by three radial strain data in 0°(ε_0), 90(°ϵ_{90}), and 135° (ϵ_{135}) as following,

$$\varepsilon(\theta) = A(\sigma_1 + \sigma_2) + B(\sigma_1 - \sigma_2)cos\, 2\theta \tag{1}$$

$$\sigma_{1,2} = \frac{1}{4A}(\varepsilon_0 + \epsilon_{90}) \pm \frac{\sqrt{2}}{4B}\sqrt{(\varepsilon_0 - \epsilon_{135})^2 + (\varepsilon_{90} - \epsilon_{135})^2} \tag{2}$$

$$tan\, 2\theta = \frac{\varepsilon_0 + \varepsilon_{90} - 2\varepsilon_{135}}{\varepsilon_0 - \varepsilon_{90}} \tag{3}$$

The strain release coefficients A and B are one of the most critical factors affecting accuracy. When using the hole-drilling method, they can be directly calculated using Kirsch theory. However, if the blind hole-drilling method is used, calibration is required due to the lack of an analytical solution. This can be achieved using the finite element method or experimental methods. The maximum relative error in the measurement results is generally considered to be about 10%.

In order to measure residual stresses by making holes on the surface of a sample, there are typically two different methods: drilling and the ring-core method. The basic principle of both methods is the release of stresses after material removal, thus both methods require at least the measurement of strains before and after hole machining. In the ring-core method, petal strain gauges are placed in the middle of the annular area, and the same formula as that used in drilling method is applied to calculate the residual stresses in that area.

Compared with drilling, the ring-core method has higher sensitivity and releases larger strains. For example, if the inner diameter of the ring is 5.6 mm, the released strain will be 90%[1]. Thus, higher accuracy can be achieved. Ajovalasit's research report[2] indicates an accuracy of 15 MPa for steel. Due to eccentricity errors tending to mutually compensate each other, the influence of the strain gauge-grinding wheel eccentricity error is also smaller than in the drilling method. Finally, the ring-core method allows measurement of stress distribution at deeper depths, even beyond 4 mm.

As precision requirements increase, the diameter of the drill holes for residual stress measurement becomes smaller. In order to overcome the spatial limitations of strain gauges, non-contact strain measurement techniques such as digital image correlation (DIC) and interferometry have recently gained attention.

When using DIC, the analysis area is first divided into several square grid images, and the displacement of the grid points is analyzed to obtain the Nelson strain field coefficient and residual stress through regression analysis. It is necessary to avoid the drilling position and not get too close to the edge of the hole. Furthermore, the accuracy is also limited by the size of the sub-image. Therefore, Baldi proposed a concept in 2014 to directly replace the traditional DIC grid displacement field with an infinite domain displacement field[3].

Baldi proposed an integrated DIC (iDIC) method that directly uses residual stress, rigid-body displacement, and exposure adjustment parameters as identification parameters. It uses the entire image as the fitting object, which can overcome the error caused by small grid size around the hole in traditional DIC algorithm and achieve measurement accuracy similar to that of interferometers. However, it does not have the problem of environmental limitations that interferometers face, and the cost is much lower than interferometer technology. Baldi's research did not use 3D measurement, which may be affected by the movement of the drilling machine and camera fixture, potentially affecting the accuracy. The main focus of this article is to propose a simple method to correct errors caused by changes in the distance between the camera and the object.

2 METHODOLOGY

2.1 Nelson Strain field integrated DIC

The integrated DIC concept was initially proposed by Roux and Hild to address the strain concentration issue encountered in DIC during stress intensity factor measurements. Its first application for residual stress measurements appeared in the research of Gao and Shang[4]. While it is similar in form to the standard local DIC method, it employs a specific shape function around the borehole (i.e., the Nelson displacement field) to describe the displacement field of the images, rather than using a generic shape function to describe how pixel blocks move and deform. This allows us to overcome the difficulties encountered by all generic programs when facing large strain gradients. In fact, by integrating the expected behavior of the specimen into the shape function, measurement bias can be entirely avoided, as there is no need to partition the region into multiple sub-regions, and a large number of pixels can be used for analysis, thus completely solving the problem of displacement standard deviation being larger than that of interferometry. Additionally, the fitting algorithm directly involves the stress components related to residual stress, allowing measurement to be performed directly without any post-processing. That is, the process is much simpler than coupling the standard DIC program with a post-fitting residual stress process.

The fundamental assumption of DIC is that the gray-scale intensity of each point on the object being imaged does not change over time and follows the equation:[5]

$$G(x, y, t) = \bar{G}(x + u_x, y + u_x, t + \Delta t) \tag{4}$$

where G and $\bar{G}$ are gray value of reference and target image respectively, $(x+u_x, y+u_y)$ is the coordinate of point (x, y) at time $t+\Delta t$, and (u_x, u_y) is the local displacement field function.

In traditional DIC, through the fitting of equation such as (4), the grayscale values at the deformed position A in the target (deformed) image should be made as similar as possible to the grayscale values at the pre-deformed position B in the reference (undeformed) image or to achieve minimum error, to represent the displacement field function to maximize their correlation. The most commonly used error function is correlation, as following

$$I_{COR}(i_0, j_0, u_x, u_y) = 1 - \frac{\sum_k \sum_l G(k,l)\bar{G}(k+u_x, l+u_y)}{\sqrt{\sum_k \sum_l G(k,l)^2 \cdot \sum_k \sum_l \bar{G}(k+u_x, l+u_y)^2}} \tag{5}$$

or square sum of error, as following

$$I_{SS}(i_0, j_0, u_x, u_y) = \sum_k \sum_l \left(G(k,l) - \bar{G}(k+u_x, l+u_y)\right)^2 \tag{6}$$

In this context, (i_0, j_0) represents the coordinate of the pixel where the measurement is performed, while u_x and u_y are the x and y displacement components to be measured. The range of k and l is within the rows (columns) of a square region centered at (i_0, j_0) (or pixels within the grid in the general case). Finally, G and $\bar{G}$ denote the grayscale values of the reference and target images, respectively, which refer to the images before and after the motion being analyzed.

In order to make A and B correspond, it is necessary to minimize the error function. This involves an iterative algorithm that makes the partial derivatives of the error function I with respect to the displacement parameters (i.e., the parameters of the shape function) approach zero. Commonly used algorithms include, for example, the Newton-Raphson algorithm or the gradient descent algorithm.

As mentioned earlier, typical DIC codes use linear (sometimes quadratic) displacement field functions. In IDIC, however, the situation is different. Since it is aimed at a well-defined problem (drilling strain fields, with a fixed displacement field type based on elasticity theory), a specific shape function can be used to describe the global (around the borehole) displacement field. Therefore, it is not necessary to perform multiple local measurements, and a true global solution can be obtained.

To adapt the general framework of DIC outlined above to the IDIC method, the general displacement function must be replaced with a specific shape function for the residual stress. In fact, the displacement field around the borehole caused by relaxation of residual stress is well-known:

$$u_r = A(\sigma_x + \sigma_y) + B[(\sigma_x - \sigma_y)\cos 2\theta + 2\tau_{xy}\sin 2\theta] \tag{7}$$

$$u_\theta = C[(\sigma_x - \sigma_y)\sin 2\theta - \tau_{xy}\cos 2\theta] \tag{8}$$

$$u_z = F(\sigma_x + \sigma_y) + G[(\sigma_x - \sigma_y)\cos 2\theta + 2\tau_{xy}\sin 2\theta] \tag{9}$$

Where u_r, u_θ and u_z are dislacements in radial, tangential and z- direction respectively.

The coefficients A, B, C, F, and G can be estimated using finite element calculations or based on theoretical solutions provided by Nelson et al.[6], as following

$$A = \frac{r_o}{2E}(1+\nu)\rho \quad B = \frac{r_o}{2E}[4\rho - (1+\nu)\rho^3] \tag{10}$$

$$C = -\frac{r_o}{2E}[2(1-\nu)\rho + (1+\nu)\rho^3]$$

$$F = 0 \quad G = \frac{\nu t}{E}\rho^2$$

where ρ is the ratio of the hole radius r_0 to the distance from the current point to the center of the hole, E is the Young's modulus, ν Poisson's ratio, t plate thickness, r, θ and z are the coordinates of the midpoint of the cylindrical reference system, and σ_x, σ_y and τ_{xy} are stress components.

Next, rigid body displacement can be added to the displacement field to take into account the relative camera motion between before and after drilling. It can be expressed as following

$$u_x(x,y,\sigma_x,\sigma_y,\tau_{xy}) = u_0 + P_u\sigma_x + Q_u\sigma_y + R_u\tau_{xy} \tag{11}$$

$$u_y(x,y,\sigma_x,\sigma_y,\tau_{xy}) = v_0 + P_v\sigma_x + Q_v\sigma_y + R_v\tau_{xy} \tag{12}$$

Here, P_u, Q_u, and R_u (P_v, Q_v, and R_v) are calibration coefficients that depend on the point's position, material properties, and the geometry of the hole, and

$$P_u = [A + (B+C)\cos 2\theta - C]\cos\theta \tag{13}$$

$$Q_u = [A - B\cos 2\theta]\cos\theta + C\sin 2\theta\sin\theta$$

$$R_u = 2[(B+C)\cos 2\theta + B]\sin\theta$$

$$P_v = [A + (B+C)\cos 2\theta + C]\sin\theta$$

$$Q_v = [A - (B+C)\cos 2\theta - C]\sin\theta$$

$$R_v = -2[(B+C)\cos 2\theta - B]\cos\theta$$

Once the displacement field around the borehole is obtained, i.e., equations (7) to (9), it can be applied in the calculation of DIC correlation coefficients (equations (5) or (6)). The calculation range is typically chosen as a region of approximately three to five times the borehole diameter around the borehole. By optimizing the identification parameters, including stress values σ_x, σ_y and τ_{xy}, as well as the rigid displacement parameters (u_0, v_0), high-precision IDIC results can be obtained. Figure 1 shows the mapping of Nelson displacement field and the calculation range in the integrated DIC.

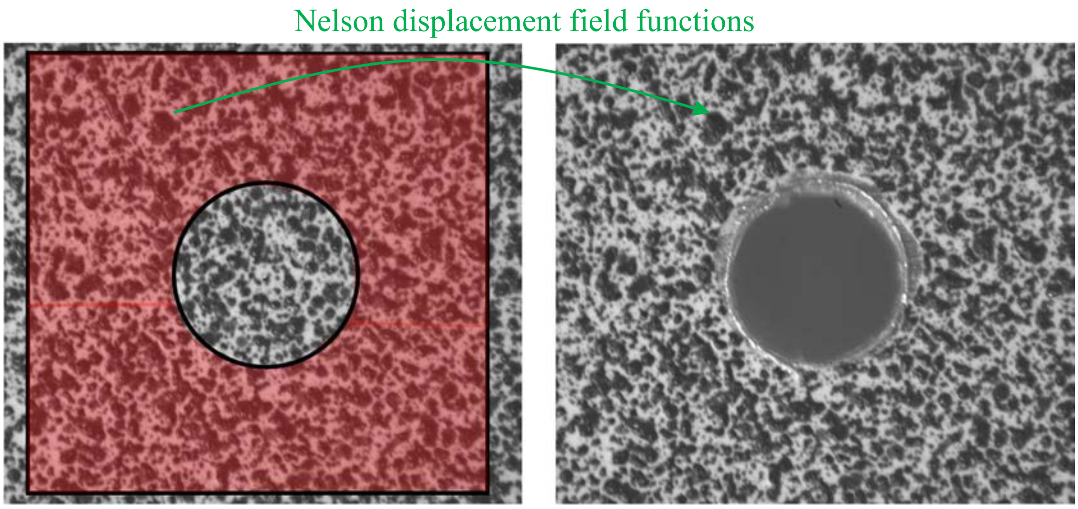

Figure 1 Concept of Nelson Strain field integrated DIC

2.2 Compensation of variance of distance between camera and object

In residual stress measurement using the hole-drilling method with DIC, a reference image must be taken before drilling a hole, then the camera is moved away, the hole is drilled, and the camera is moved back to take a target image. This process causes a change in the distance between the camera and the specimen, a phenomenon called "shooting distance effect" may occur, which leads to the generation of false strain when there is a change in the distance between the camera and the test object. The reason for this effect is that the change in distance affects the size and shape of pixels, resulting in errors in strain calculation. To solve this problem, one can try to keep the distance between the camera and the test object stable during the reference and target image capture, or use some correction methods to eliminate this effect. Therefore, in the residual stress measurement using the hole-drilling method, one should be aware of the shooting distance effect and choose appropriate solutions to ensure the accuracy and reliability of the measurement results.

Among various methods, three-dimensional image measurement is a way to more precisely correct false strain. However, due to the limitation of experimental space, it is difficult to implement three-dimensional measurement using multiple cameras, especially when using a microscopic camera. Therefore, this article proposes a simplified method to achieve the same effect.

When the tested object remains stationary, the camera is forced to perform a translation perpendicular to the normal vector of the tested object surface. According to the research of Shih et al.[7], the relative length of the image coordinate vector of any point in the images captured before and after the translation is inversely proportional to the distance between that point and the camera lens. Using this relationship, it is possible to detect the change rate of the camera-object distance before and after drilling and obtain the magnitude of the fictitious strain, which can be used to compensate for the strain error caused by the "photographic distance effect." Based on this principle, this study proposes a simple correction procedure for pseudo-strain as follows:

Step-1: Fix the camera on a single-axis translation stage with an accuracy of 0.001mm.

Step-2: Adjust the direction of the translation stage's main axis to be perpendicular to the surface normal vector of the test object, allowing for an error of less than 5 arcminutes.

Step-3: Take the first reference image (Img_Ref_1) by positioning the camera at the expected drilling location.

Step-4: Move the camera 2mm by forcing the camera to translate using the translation stage and take the second reference image (Img_Ref_2).

Step-5: Drill the hole after moving the camera away.

Step-6: Move the camera back to the drilling location and take the first target image (Img_Tar_1) by positioning the camera at the center of the hole.

Step-7: Move the camera 2mm by forcing the camera to translate using the translation stage and take the second target image (Img_Tar_2).

Step-8: Select several points (at least four) distributed around the drilling hole from Img_Ref_1. Analyze their coordinates in Img_Ref_2, and calculate their displacement (in pixels) as the ΔL_{Ref}

Step-9: Analyze the coordinates of the points from Step 8 in Img_Ref_1 and Img_Ref_2, and calculate their relative displacement (in pixels) as the ΔL_{Tar}

Step-10: Calculate the fictitious strain using the following equation:

$$\delta\varepsilon = \frac{\Delta L_{Ref}}{\Delta L_{Tar}} - 1 \quad (14)$$

Finally, the normal strain obtained from the IDIC analysis between the first reference image and the first target image can be corrected by subtracting the fictitious strain obtained from Equation (14), resulting in a more accurate measurement of normal strain.

3 EXPERIMENTAL VALIDATION

The first page must contain the Title, Author(s), Affiliation(s), Key words and the Summary. The Introduction must begin immediately below, following the format of this template.

3.1 Experimental Setup

The experimental process includes four steps: capturing a reference image under no load, capturing a post-deformation image after applying tension, drilling a hole, and capturing a post-drilling image. In this study, a custom-designed testing apparatus was used to facilitate these steps while maintaining a suitable distance between the camera and specimen as much as possible.

The experiment setup as shown in Figure 2 including:

- a industrial digital camera of Basler (Basler acA5472-17uc) with resolution of 5472x3648.
- a microscope lens of Navitar Zoom 6000 series lens with magnification ratio of 0.7x~4.7x. In the experiment, the magnification ratio is set as 3x.
- a three-axis platform equipped with a dial gauge with a resolution of 0.001 mm.
- a drilling machine with a speed of 10,000 rpm.

Figure 2 Experimental setup

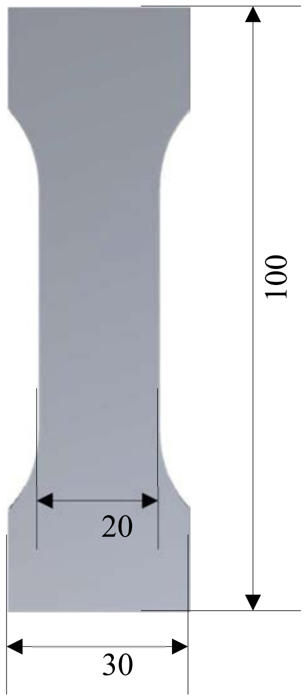

Figure 3 Specimen details (Al. alloy)

3.2 Specimen details

This experiment produced three tensile specimens with dimensions of 100x50x3mm and made of aluminum alloy (6000 Series). The dimensions of each part of the specimens are shown in Figure 3.

3.3 Experimental result

A. Verification of the applicability of the Nelson displacement field

After the optimization of the correlation coefficients, the current stress state and rigid body displacement vectors that best match the post-drilling image were obtained. To validate the accuracy of the results, an inverse transformation was performed by substituting the identified current stress state and rigid body displacement vectors into equations (11) and (12) to generate a simulated virtual post-drilling image from the pre-drilling image. This image was then superimposed onto the real post-drilling image, as shown in Figure 4. The high degree of similarity between the two images in Figure 4 provides strong evidence for the suitability of the Nelson displacement field and the high precision of the identified current stress state.

B. Validation of the accuracy of current stress state

As a validation standard for the accuracy of Nelson-IDIC current stress, high-precision strain values at the hole location are required. Due to the size limitations of the test specimen, the stress field cannot be guaranteed to be uniform, and direct measurement of the force and dividing by the average stress of the cross-section may not represent the current stress at the hole location. Therefore, in this study, a generic pattern DIC analysis was conducted using the pre-loading image as the reference image and the pre-drilling image after loading as the target image to obtain the most realistic current strain distribution and the average strain at the drilling location.

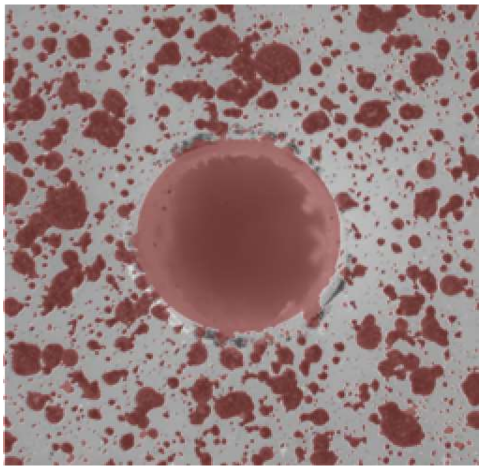

Figure 4 Virtual post-drilling image superimposed onto the real post-drilling image

Without compensation for the fictitious strain, the measured average strain at the drilled hole location were $\bar{\varepsilon}_{xx} = 0.00130$, $\bar{\varepsilon}_{yy} = 0.00001$, $\bar{\gamma}_{xy} = 0.00015$. After the correction of the fictitious strain, the average strain at the drilled hole location are $\varepsilon_{xx}^{cal} = 0.002019$, $\varepsilon_{yy}^{cal} = 0.000627$, $\gamma_{xy}^{cal} = 0.000150$, and the stress states are

$$\begin{Bmatrix} \sigma_{xx}^{cal} \\ \sigma_{yy}^{cal} \\ \tau_{xy}^{cal} \end{Bmatrix} = \frac{E}{1-\nu^2} \begin{bmatrix} 1 & \nu & 0 \\ \nu & 1 & 0 \\ 0 & 0 & \dfrac{1-\nu^2}{2(1+\nu)} \end{bmatrix} = \begin{Bmatrix} 174.89 \\ 101.16 \\ -3.95 \end{Bmatrix} MPa \tag{15}$$

The current state stress identified by Nelson IDIC at the drilled hole position were

$$\begin{Bmatrix} \sigma_{xx}^{IDIC} \\ \sigma_{yy}^{IDIC} \\ \tau_{xy}^{IDIC} \end{Bmatrix} = \begin{Bmatrix} 167.05 \\ 99.73 \\ -4.39 \end{Bmatrix} MPa \tag{16}$$

After correction of the fictitious stress, the corrected current state stress is as following

$$\begin{Bmatrix} \sigma_{xx}^{m} \\ \sigma_{yy}^{m} \\ \tau_{xy}^{m} \end{Bmatrix} = \begin{Bmatrix} 177.64 \\ 110.31 \\ -4.39 \end{Bmatrix} MPa \tag{17}$$

Comparing equations (15) and (17), it can be observed that the measured values of the current stresses after the phantom stress correction show a high degree of agreement with the true values, with measurement errors of only 1.57% for normal stresses in the x-direction, -1.40% for normal stresses in the y-direction, and 11.1% for shear stresses. The error percentage for shear stresses appears to be larger because of their relatively low magnitude.

4 CONCLUSIONS

In this study, a Nelson-integrated DIC (IDIC) software was developed with theoretical corrections to account for rigid body motion. Experimental validation on aluminum alloy tensile specimens demonstrated that the proposed improvements can achieve high-precision current stress measurements. Specific conclusions can be drawn as followings:

(1) The current stress measurements using the hole-drilling method show good agreement with the pre-drilled stress measured by DIC. The main stress measurement error, σ_{xx}, is 2.74 MPa, only 1.57% of the reference stress. The measurement error for the smaller shear stress is -0.44 MPa.

(2) When using Nelson-IDIC for current stress identification, compensation for fictitious stress due to the shooting distance effect is necessary. Otherwise, an accurate results for stresses below the yield stress cannot be achieved.

(3) The camera shifting method proposed in this study can measure fictitious stress, which is an important step in the IDIC process.

5 ACKNOWLEDGEMENT

This research was supported by the National Science and Technology Commission of Taiwan under grant numbers MOST 110-2221-E-260-004 and MOST 110-2221-E-260-004. We would like to express our sincere appreciation for their support.

REFERENCES

[1] Misra, A. and Peterson, H. A. (1981), Examination of the ring method for determination of residual stresses. Exp Mech., 21(7):268–72.
[2] Ajovalasit, A., Petrucci, G. and Zuccarello, B. (1996), Determination of nonuniform residual stresses using the ring-core method. J Eng Mater Tech, 224–8.
[3] Baldi, A. (2014), Residual Stress Measurement Using Hole Drilling and Integrated Digital Image Correlation Techniques, Experimental Mechanics, Vol. 54, pages 379-391.
[4] Gao J., Shang H. (2009), Deformation-pattern-based digital image correlation method and its application to residual stress measurement. Appl Optics 48(7):1371–1381.
[5] Chu, T.C., Ranson, W.F., Sutton, M.A. and Peters, W.H. (1985), Applications of Digital-Image-Correlation Techniques to Experimental Mechanics, Exp. Mech., September, 1985, pages:232-244.
[6] Nelson D.V., Makino A., Fuchs E.A. (1997), The holographic-hole drilling method for residual stress determination. Optics Lasers Eng. 27:3–23.
[7] Tung, S.-H., Shih, M.-H. (2011), Precision verification of a simplified three-dimensional DIC method, Optics and Lasers in Engineering, Volume 49, Issue 7, Pages 937-945.